

Switching the Top Slice of the Sandwich with Extra Filling Yields a Stronger Boomerang for NLFSR-based Block Ciphers

Amit Jana¹, Mostafizar Rahman², Dhiman Saha³, Goutam Paul¹

¹Cryptology and Security Research Unit (CSRU),
R. C. Bose Centre for Cryptology and Security,
Indian Statistical Institute Kolkata
janaamit001@gmail.com, goutam.paul@isical.ac.in

²University of Hyogo

mrahman454@gmail.com

³de.ci.phe.red LAB,

Department of Computer Science & Engineering,
Indian Institute of Technology Bhilai

dhiman@iitbhilai.ac.in

Abstract. The Boomerang attack was one of the first attempts to visualize a cipher (E) as a composition of two sub-ciphers ($E_0 \circ E_1$) to devise and exploit two high-probability (say p, q) shorter trails instead of relying on a single low probability (say s) longer trail for differential cryptanalysis. The attack generally works whenever $p^2 \cdot q^2 > s$. However, it was later succeeded by the so-called “sandwich attack” which essentially splits the cipher in three parts $E'_0 \circ E_m \circ E'_1$ adding an additional *middle* layer (E_m) with distinguishing probability of $p^2 \cdot r \cdot q^2$. It is primarily the generalization of a body of research in this direction that investigate what is referred to as the *switching* activity and capture the dependencies and potential incompatibilities of the layers that the middle layer separates. This work revisits the philosophy of the sandwich attack over multiple rounds for NLFSR-based block ciphers and introduces a new method to find high probability boomerang distinguishers. The approach formalizes boomerang attacks using only ladder/And switches. The cipher is treated as $E = E_m \circ E_1$, a specialized form of a sandwich attack which we called as the “open-sandwich attack”. The distinguishing probability for this attack configuration is $r \cdot q^2$.

Using this innovative approach, the study successfully identifies a deterministic boomerang distinguisher for the keyed permutation of the Tiny-Jambu cipher over 320 rounds. Additionally, a 640-round boomerang with a probability of 2^{-22} is presented with 95% success rate. In the related-key setting, we unveil full-round boomerangs with probabilities of 2^{-19} , 2^{-18} , and 2^{-12} for all three variants, demonstrating a 99% success rate. Similarly, for KATAN32, a more effective related-key boomerang spanning 140 rounds with a probability of 2^{-15} is uncovered with 70% success rate. Further, in the single-key setting, a 84 round boomerang with probability 2^{-30} found with success rate of 60%. This research deepens the understanding of boomerang attacks, enhancing the toolkit for cryptanalysts to develop efficient and impactful attacks on NLFSR-based block ciphers.

45 **Keywords:** MILP · Boomerang · Sandwich · KATAN · TinyJAMBU ·
46 Symmetric-Key Cryptanalysis

47 1 Introduction

48 The introduction of the Boomerang attack by Wagner [22] was an important
49 moment in the history of block cipher cryptanalysis. This was primarily because
50 it allowed us to interpret a cipher as a composition of sub-ciphers showcasing
51 the interaction of differential trails on orthogonal planes of the *Boomerang-Cube*.
52 This demonstrated that shorter (and hence high probability) trails on orthogo-
53 nal plane of the sub-ciphers were better than longer (and hence low probability)
54 rails on a single plane of the full block cipher. Thus was born the ‘*Boomerang*
55 *Quartet*’ whose analysis spawned an entire body of research giving us further
56 insight into *Boomerang-Cube* and its exploitation to deliver some of the best
57 distinguishers on block ciphers reported in literature. In the classical boomerang
58 attack, the cipher E is considered as a composition of two sub-ciphers E_0 and E_1 ,
59 i.e., $E = E_1 \circ E_0$, where we suppose that the input difference Δ_0 is propagated to
60 the difference Δ_1 by E_0 with probability p and the difference ∇_0 is propagated
61 to ∇_1 by E_1 with probability q . This is described in Figure 1 while the expected
62 probability of this attack is shown below. Equation 1 shows that by performing
63 $\frac{1}{p^2 \cdot q^2}$ number of adaptively chosen plaintext/ciphertext queries with the Δ_0 differ-
64 ence on the encryption queries and the ∇_1 difference on the decryption queries,
65 the attacker can distinguish E from the ideal cipher. The most important part of
66 this boomerang-style attacks is to select suitable differential characteristics for
67 E_0 and E_1 so that the probability of obtaining a right quartet will be maximized.
68 Also, in this type of attacks, the overall probability was calculated based on the
69 assumption that the two sub-ciphers E_0 and E_1 are independent.

$$\Pr[E^{-1}(E(x) \oplus \nabla_1) \oplus E^{-1}(E(x \oplus \Delta_0) \oplus \nabla_1) = \Delta_0] = p^2 \cdot q^2. \quad (1)$$

70 One direction in boomerang research entailed improving the boomerang trails
71 by the relaxing the assumptions at the edge of the sub-ciphers (like the Amplified
72 Boomerang [17] attack) while another attempt was to convert the Boomerang
73 attack to a chosen plaintext attack (Rectangle Attack [3]) with the penalty of an
74 increased complexity. Yet another direction was inspired by Murphy’s work [18]
75 on the impossible Boomerang Quartet (showing incompatibilities between upper
76 and lower trails due to incorrectness of the independence assumption). Research
77 in this direction lead to many interesting contributions which let to the plane
78 at the edge of the sub-ciphers in the Boomerang-Cube to be inflated to a cube
79 in itself. This view allowed capture the various dependencies between the upper
80 and lower trails and also resolved the problem of incompatible trails.

81 *Research Exploiting Inter-trail Dependencies in the Boomerang-Cube* One of
82 the first exploitations of trail dependencies was due to Biryukov et al. in the
83 middle round S-box trick [5]. Besides, many improvements taking advantages of
84 the dependency between the two differential characteristics have been proposed,

85 such as the ladder switch, S-box switch, and the Feistel switch in [6]. The basic
 86 idea is that the boundaries of E_0 and E_1 do not need to be defined on a state,
 87 instead, the state can be further divided into words, and some words can be in
 88 E_0 and others can be in E_1 . Suppose, in a boomerang trail, half of the state
 89 is active in the upper trail E_0 , the other half is active in the lower trail E_1 , in
 90 between them only S-box layer is there. In this case, the probability on all the
 91 active S-boxes becomes 1. This technique is called ladder switch. Further, in the
 92 S-box switch, when both the characteristics for E_0 and E_1 activate the same
 93 S-box with an identical input difference and an identical output difference, the
 94 probability of this S-box to generate a quartet becomes p' instead of p'^2 .

95 Later, in [12,13], Dunkelman et al. formalised the above observations, and
 96 captured in the framework of sandwich attack. In this attack, the target cipher
 97 E can be further decomposed into three parts, i.e., $E = E_1 \circ E_m \circ E_0$ where
 98 the middle part E_m consists of relatively short transformations (as depicted in
 99 Figure 2). Let (x_1, x_2, x_3, x_4) and (y_1, y_2, y_3, y_4) be the input and the output
 100 quartet values for E_m respectively such that $y_i = E_m(x_i)$. Thus, the probability
 101 of a valid boomerang quartet would be $p^2 \cdot q^2 \cdot r$, where r denotes the probability
 102 of E_m satisfying some differential propagation among four texts and is computed
 103 as follows.

$$r = \Pr[(x_3 \oplus x_4 = \Delta_1) | (x_1 \oplus x_2 = \Delta_1) \wedge (y_1 \oplus y_3 = \nabla_0) \wedge (y_2 \oplus y_4 = \nabla_0)]. \quad (2)$$

104 Therefore, the boomerang switching effects can be integrated as the dependency
 105 between the two characteristics of E_0 and E_1 which now lie in E_m . To
 106 calculate the probability r of E_m in a systematic way, as well as for finding the
 107 other switches to increase r , Cid et al. in [9] first proposed an efficient technique,
 108 called Boomerang Connectivity Table (BCT) to capture the boomerang switches
 109 of E_m . The BCT can capture both the incompatibility, introduced by [18] and
 110 the observations by [6]. Moreover, BCT shows that the switching effect can be ap-
 111 plied to increase the probability even when Δ_1 cannot be propagated to Δ_2 in the
 112 DDT. The drawbacks of BCT is that the incompatibility can be avoided by upto
 113 one round, but it cannot capture the incompatibility when multiple rounds of E_m
 114 are considered. In [23], Wang et al. proposed a modified tool, called Boomerang
 115 Difference Table (BDT) to improve the BCT when considering multiple rounds.
 116 Several other improvements on the middle layer for boomerang switch can be
 117 found in [21,26].

118 *NLFSR-based Designs.* Securing low-end devices like RFID tags is challenging due
 119 to their constrained environment. The ideal security solution must be compact,
 120 low-power, and fast enough for real-time protocols. In this context, NLFSR-based
 121 designs are a suitable choice. They offer several advantages such as low hardware
 122 cost, efficient parallel computation of rounds, and easy loading of stream input
 123 data into the state during state updates. These characteristics make NLFSR-
 124 based designs well-suited for compact, low-power, and real-time protocol require-
 125 ments. Some well-known NLFSR-based designs include Grain, Trivium, KATAN,
 126 and TinyJambu. In we demonstrate the application of generalized boomerang

127 switch techniques on the NLFSR-based block cipher KATAN, which is a highly
128 efficient hardware-oriented cipher. Additionally, we explore the keyed permuta-
129 tion of TinyJambu, which was one of the ten finalists in the NIST lightweight
130 authenticated encryption competition [2].

131 1.1 Our Contributions

132 Our contributions in this work can be summarized as follows:

- 133 – **Comprehensive Analysis of Switching Techniques for NLFSR-based ciphers:** We
134 provide a comprehensive analysis of boomerang attacks, particularly in the
135 context of NLFSR-based ciphers. By investigating the impact of different
136 switch techniques, we deepen the understanding of how these attacks work
137 and how the interdependencies between characteristics influence their suc-
138 cess.
- 139 – **Introducing the Open-Sandwich Attack:** We introduce a novel approach to
140 identify boomerang distinguishers by exclusively utilizing the path through
141 ladder or And switches. This approach, called as the “open-sandwich attack”,
142 offers a new perspective on attack modeling and provides a new way to
143 uncover vulnerabilities in ciphers.
- 144 – **Best distinguishers on TinyJambu and KATAN32:** Using our approach, we suc-
145 cessfully identify better boomerang distinguishers for ciphers, like TinyJambu
146 and KATAN32. A brief comparison of these attacks are presented in Table 1.
147 These discoveries highlight the practical applicability of our methods and
148 their potential to uncover weaknesses in real-world cryptographic systems.

149 1.2 Outline of the Paper

150 The structure of this paper is outlined as follows. In Section 2, we establish the
151 foundational knowledge necessary for constructing a novel sandwich attack tai-
152 lored for NLFSR-based block ciphers. Section 3 is dedicated to a comprehensive
153 discussion on the development of a Mixed Integer Linear Programming (MILP)
154 model, effectively dissecting the sandwich attack through the utilization of var-
155 ious switches. Section 4 presents empirical results derived from our innovative
156 technique, applied to both the related-key and single-key settings for the Tiny-
157 Jambu cipher. Additionally, Section 5 extends our methodology to explore and
158 discover optimal boomerangs for the KATAN32 cipher under both key settings.
159 Subsequently, in Section 6, we engage in a discussion encompassing potential en-
160 hancements and future research challenges pertinent to our technique. Finally,
161 Section 7 offers concluding remarks that summarize the key findings and impli-
162 cations of our work.

163 2 Preliminaries

164 In this section, we begin by providing a concise overview of the framework of
165 boomerang attacks. Following that, we delve into the categorization of the gener-
166 alized switching effects for a single AND-based non-linear feedback shift register

Table 1: Comparison of Attacks against KATAN32 and TinyJambu variants. Here SK, RK, KP, ACP represent Single-key, Related-key, Known Plaintext and Adaptive Chosen Plaintext respectively

Cipher	Techniques	Attack Model	Key Size	Rounds	Distinguishing Probability	References	
TinyJambu	Differential	RK	128	1024	2^{-16}	[11]	
					2^{-14}	[16]	
			192	1152	2^{-12}	[11]	
					2^{-10}	[16]	
		256	1280	2^{-10}	[11]		
				2^{-8}	[16]		
		SK	128		384	2^{-19}	[19]
					384	2^{-14}	[16]
	640				2^{-42}		
	1024				2^{-108}		
	Slide	KP	128	∞	2^{-64}	[20]	
		ACP	192	∞	2^{-65}		
		ACP	256	∞	$2^{-67.5}$		
	Boomerang	RK		128	1024	2^{-19}	This Work Section 5
192				1152	2^{-18}		
256				1280	2^{-12}		
SK		128	640	2^{-22}			
KATAN32	Boomerang	RK	80	140	$2^{-27.2}$	[15]	
					$2^{-26.58}$	[8]	
					2^{-15}	This Work Section 6	
		SK	80	83†	$2^{-21.78}$	[8]	
				84	2^{-30}	This Work Section 6	

†The given trail has probability much lower than 2^{-32} .

167 (NLFSR). This discussion aims to lay the foundation for a comprehensive under-
168 standing of boomerang attacks and their applicability in cryptographic analysis.

169 **2.1 Differential Propagation through AND Gates**

170 Differential cryptanalysis was first proposed by Biham and Shamir in the early
 171 1990s in [4]. It is one of the most fundamental cryptanalytic approach to eval-
 172 uate the security of block ciphers. For differential cryptanalysis, the basic idea
 173 is to find the higher probability differential trails by assuming that the state
 174 differences spreading through the rounds in a cipher are independent. This prob-
 175 ability comes due to some active non-linear components through the rounds for
 176 iterated ciphers, and is inversely proportional to the number of rounds. Thus,
 177 the resistance against differential cryptanalysis for iterated ciphers (based on
 178 the non-linear components like S-box/Addition/AND operations) is highly de-
 179 pendent on the non-linearity features of these operations. For an n -bit S-box
 180 $S : \{0, 1\}^n \rightarrow \{0, 1\}^n$, the differential properties of S are typically represented
 181 by the $2^n \times 2^n$ Difference Distribution Table (DDT) T , where a row represents
 182 the input difference (Δ_i) and a column represents the output difference (Δ_o).
 183 The entries in T are defined by $T(\Delta_i, \Delta_o) = \#\{x : S(x) \oplus S(x \oplus \Delta_i) = \Delta_o\}$.

184 Thus, the probability for any given difference pair (Δ_i, Δ_o), i.e., the input dif-
 185 ference Δ_i propagates to the output difference Δ_o is $\frac{T(\Delta_i, \Delta_o)}{2^n}$. Also, for an AND
 186 gate, if $(\Delta a, \Delta b)$ denotes the input difference and Δz as its output difference,
 187 then we have,

$$\Delta z = a \cdot b \oplus (a + \Delta a) \cdot (b + \Delta b) = a \cdot \Delta b \oplus b \cdot \Delta a \oplus \Delta a \cdot \Delta b. \quad (3)$$

188 The differential properties of AND gate can also be represented by 4×2 DDT
 189 table T , which is given in Table 2. The entries in the table T are defined by

$$T((\Delta a, \Delta b), \Delta z) = \#\{(a, b) : a \cdot b \oplus (a \oplus \Delta a) \cdot (b \oplus \Delta b) = \Delta z\}.$$

$(\Delta a, \Delta b)$	$\Delta z = 0$	$\Delta z = 1$
(0, 0)	4	0
(0, 1)	2	2
(1, 0)	2	2
(1, 1)	2	2

Table 2: Difference Distribution Table of AND Gate

190 Therefore, the probability for the input difference $(\Delta a, \Delta b)$ propagates to
 191 the output difference Δz will be $\frac{T((\Delta a, \Delta b), \Delta z)}{4}$. According to the Table 2, the
 192 output difference Δz follows a uniform distribution for any given non-zero input
 193 difference $(\Delta a, \Delta b)$.

194

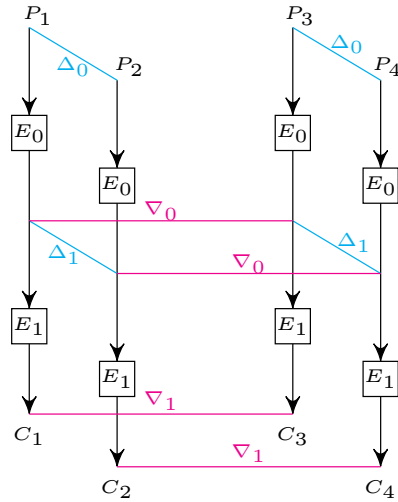


Fig. 1: Boomerang Attack

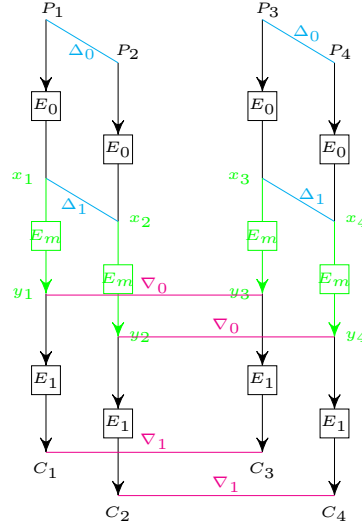


Fig. 2: Sandwich Attack

195 2.2 Boomerang Attack

196 Now, we give a brief overview of the boomerang attack. Let $E_K(P)$ and $E_K(C)$
 197 denote the encryption of P and the decryption of C under a key K , respectively.
 198 Suppose $\Delta K, \nabla K$ are the master key differences of the differentials. Then, the
 199 boomerang distinguisher is mounted as follows:

- 200 1. Ask for the ciphertexts $C_1 = E_K(P_1)$ and $C_2 = E_K(P_2)$, where $P_2 = P_1 \oplus \Delta_0$.
- 201 2. Ask for the plaintexts $P_3 = E_K^{-1}(C_3)$ and $P_4 = E_K^{-1}(C_4)$, where $C_3 = C_1 \oplus \nabla_1$
 202 and $C_4 = C_2 \oplus \nabla_1$.
- 203 3. Check whether $P_3 \oplus P_4 = \Delta_0$.

204 Also, the boomerang framework in the related-key setting works as follows:

- 205 1. $K_1 \leftarrow K, K_2 \leftarrow K_1 \oplus \Delta K, K_3 \leftarrow K_1 \oplus \nabla K, K_4 \leftarrow K_1 \oplus \Delta K \oplus \nabla K$.
- 206 2. Ask for the ciphertexts $C_1 = E_{K_1}(P_1)$ and $C_2 = E_{K_2}(P_2)$, where $P_2 =$
 207 $P_1 \oplus \Delta_0$.
- 208 3. Ask for the plaintexts $P_3 = E_{K_3}^{-1}(C_3)$ and $P_4 = E_{K_4}^{-1}(C_4)$, where $C_3 =$
 209 $C_1 \oplus \nabla_1$ and $C_4 = C_2 \oplus \nabla_1$.
- 210 4. Check whether $P_3 \oplus P_4 = \Delta_0$.

211 **Switching in Boomerang Attacks.** Here, we give a brief overview of the
 212 switching techniques that are employed in the boomerang attacks tailored for
 213 Substitution-Permutation Network (SPN) based ciphers. Consider a cipher E

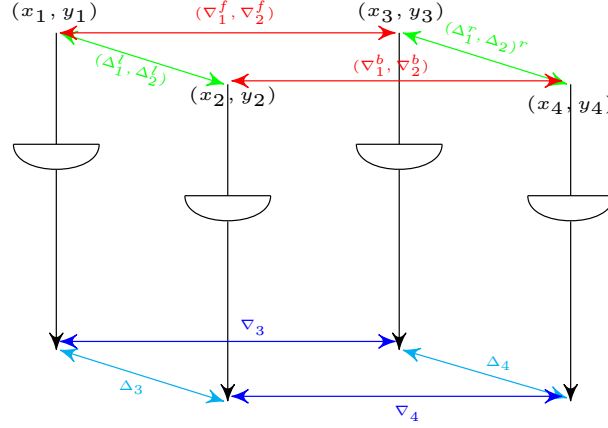


Fig. 3: A Valid Boomerang Quartet of E_m as One Round NLFSR

214 and its decomposition $E = E_1 \circ E_m \circ E_0$ (refer to Fig. 2) as formalised in [12,13].
 215 Assume that the last substitution layer partitions x_1 into t words, i. e., $x_1 =$
 216 $x_1^0 || \dots || x_1^{t-1}$. Similarly, x_i 's ($2 \leq i \leq 4$), y_j 's ($1 \leq j \leq 4$), Δ_1 and ∇_0 can be
 217 partitioned into t words (assume that the corresponding s-box is $\nu \times \nu$). Consider
 218 the following relation for the k -th word-

$$x_1^{k-1} \oplus x_2^{k-1} = \Delta_1^{k-1}$$

219 For satisfying the E_0 trail (in the return path of the boomerang), the following
 220 relation must hold for $1 \leq k \leq t$ -

$$S^{-1}(S(x_1^{k-1}) \oplus \nabla_0^{k-1}) \oplus S^{-1}(S(x_2^{k-1}) \oplus \nabla_0^{k-1}) = \Delta_1^{k-1} \quad (4)$$

221 where S is the substitution operation applied on each word. Now consider
 222 the following two cases-

- 223 – **Case I:** When $x_1^{k-1} = x_2^{k-1}$, Eq. 4 holds with probability one. This particular
 224 case is designated as *ladder* switch.
- 225 – **Case II:** When $S(x_1^{k-1}) \oplus S(x_2^{k-1}) = \nabla_0^{k-1}$, Eq. 4 holds with probability $\frac{\mu}{2^\nu}$,
 226 where μ is entry in the difference distribution table (DDT) of S with Δ_1^{k-1}
 227 and ∇_0^{k-1} as the input and output differences, respectively. This particular
 228 case is designated as s-box switch.

229 Next, we introduce a notion similar to these switches when the non-linear
 230 layer of a cipher consists of AND operations.

231 3 Introducing Generalized Switching in NLFSR

Consider the middle layer E_m in a sandwich attack which is composed of a
 single round NLFSR-based cipher which has only one AND gate as the non-linear

		(∇_1, ∇_2)			
		$(0,0)$	$(1,0)$	$(0,1)$	$(1,1)$
(Δ_1, Δ_2)	$(0,0)$	4	4	4	4
	$(1,0)$	4	4	0	0
	$(0,1)$	4	0	4	0
	$(1,1)$	4	0	0	4

Table 3: Boomerang Connectivity Table of Single AND-based NLFSR

component, given in Figure 3. The target cipher is divided into three parts E_0 , E_m , and E_1 . Let $(x_1, y_1), (x_2, y_2), (x_3, y_3), (x_4, y_4) \in \{0, 1\}^2$ are the inputs to the four AND gates of E_m such that $x_1 \oplus x_2 = x_3 \oplus x_4 = \Delta_1^l = \Delta_1^r = \Delta_1$ (say), $y_1 \oplus y_2 = y_3 \oplus y_4 = \Delta_2^l = \Delta_2^r = \Delta_2$, $x_1 \oplus x_3 = x_2 \oplus x_4 = \nabla_1^f = \nabla_1^r = \nabla_1$ and $y_1 \oplus y_3 = y_2 \oplus y_4 = \nabla_2^f = \nabla_2^r = \nabla_2$. Also, let $z_1, z_2, z_3, z_4 \in \{0, 1\}$ are the corresponding output differences such that $z_1 \oplus z_2 = \Delta_3$ and $z_3 \oplus z_4 = \Delta_4$. For $(x, y) \in \{0, 1\}^2$, the output difference of the AND operation in the left plane is given by

$$\Delta_3 = x \cdot y \oplus (x \oplus \Delta_1) \cdot (y \oplus \Delta_2).$$

Similarly,

$$\Delta_4 = (x \oplus \nabla_1) \cdot (y \oplus \nabla_2) \oplus (x \oplus \nabla_1 \oplus \Delta_1) \cdot (y \oplus \nabla_2 \oplus \Delta_2).$$

232 In order to obtain a right quartet, we can obtain a necessary condition similar
 233 to Equation 4 for such NLFSR-based ciphers-

$$\begin{aligned} \Delta_3 &= \Delta_4 \\ \implies x \cdot y \oplus (x \oplus \Delta_1) \cdot (y \oplus \Delta_2) &= (x \oplus \nabla_1) \cdot (y \oplus \nabla_2) \oplus (x \oplus \nabla_1 \oplus \Delta_1) \cdot (y \oplus \nabla_2 \oplus \Delta_2) \end{aligned}$$

234 Then, the probability that the above condition holds is given by:

$$\begin{aligned} Pr[\Delta_3 = \Delta_4] \\ = \frac{\#\{(x, y) : (x \oplus \nabla_1) \cdot (y \oplus \nabla_2) \oplus ((x \oplus \Delta_1) \oplus \nabla_1) \cdot ((y \oplus \Delta_2) \oplus \nabla_2) = (x \cdot y) \oplus ((x \oplus \Delta_1) \cdot (y \oplus \Delta_2))\}}{2^2} \end{aligned} \quad (5)$$

235 The evaluation of Equation 5 is illustrated in Figure 2. This is exactly the
 236 r in Equation 2, when E_m is a single AND layer. Similar to the DDT, we eval-
 237 uate the Boomerang Connectivity Table (BCT) using Equation 5 for all pairs
 238 of (Δ_1, Δ_2) and (∇_1, ∇_2) as shown in Table 3. Further, according to Figure 3
 239 different generalized switching techniques are introduced here.

240 TRIVIAL SWITCH:

$$\{\Delta_3 = \Delta_4 = \nabla_3 = \nabla_4 = 0 \quad \text{if } (\Delta_1^l, \Delta_2^l) = (\Delta_1^r, \Delta_2^r) = (\nabla_1^f, \nabla_2^f) = (\nabla_1^b, \nabla_2^b) = (0, 0).\}$$

241 LADDER SWITCH:

$$\begin{cases} \Delta_3 = \Delta_4 = 0, \nabla_3 = \nabla_4 & \text{if } (\Delta_1^l, \Delta_2^l) = (\Delta_1^r, \Delta_2^r) = (0, 0), (\nabla_1^f, \nabla_2^f) = (\nabla_1^b, \nabla_2^b) \neq (0, 0), \\ \Delta_3 = \Delta_4, \nabla_3 = \nabla_4 = 0 & \text{if } (\Delta_1^l, \Delta_2^l) = (\Delta_1^r, \Delta_2^r) \neq (0, 0), (\nabla_1^f, \nabla_2^f) = (\nabla_1^b, \nabla_2^b) = (0, 0). \end{cases}$$

242 AND SWITCH:

$$\{\Delta_3 = \Delta_4 = \nabla_3 = \nabla_4 \quad \text{if } (\Delta_1^l, \Delta_2^l) = (\Delta_1^r, \Delta_2^r) = (\nabla_1^f, \nabla_2^f) = (\nabla_1^b, \nabla_2^b) \neq (0, 0).$$

243 TRAIL SWITCH:

$$\begin{cases} \Delta_3 \neq \Delta_4, \nabla_3 \neq \nabla_4 & \text{if } (\Delta_1^l, \Delta_2^l) = (\Delta_1^r, \Delta_2^r) \neq (0, 0), \\ & (\nabla_1^f, \nabla_2^f) = (\nabla_1^b, \nabla_2^b) \neq (0, 0), (\Delta_1^l, \Delta_2^l) \neq (\nabla_1^f, \nabla_2^f), \\ \Delta_3 = \Delta_4, \nabla_3 \neq \nabla_4 & \text{if } (\Delta_1^l, \Delta_2^l) = (\Delta_1^r, \Delta_2^r), (\nabla_1^f, \nabla_2^f) \neq (\nabla_1^b, \nabla_2^b), \\ \Delta_3 \neq \Delta_4, \nabla_3 = \nabla_4 & \text{if } (\Delta_1^l, \Delta_2^l) \neq (\Delta_1^r, \Delta_2^r), (\nabla_1^f, \nabla_2^f) = (\nabla_1^b, \nabla_2^b), \\ \Delta_3 \neq \Delta_4, \nabla_3 \neq \nabla_4 & \text{if } \begin{cases} (\Delta_1^l, \Delta_2^l) \neq (\Delta_1^r, \Delta_2^r), (\nabla_1^f, \nabla_2^f) \neq (\nabla_1^b, \nabla_2^b), \\ (\Delta_1^l, \Delta_2^l) = (\Delta_1^r, \Delta_2^r) \neq (\nabla_1^f, \nabla_2^f) = (\nabla_1^b, \nabla_2^b). \end{cases} \end{cases}$$

244 In the context of distinguishing probability, the various switches play a sig-
 245 nificant role within the framework of the boomerang attack. The objective in
 246 forming a boomerang quartet is to maintain equal parallel plane (state) differ-
 247 ences in both the segments. Considering a one-round operation denoted as E_m
 248 (refer to Figure 3), and omitting the shifting operation within the state, taking
 249 a special case where $\Delta_1^l = \Delta_1^r$, $\Delta_2^l = \Delta_2^r$, $\nabla_1^f = \nabla_1^b$, and $\nabla_2^f = \nabla_2^b$, the probabili-
 250 ties for the corresponding output differences that will be the same under these
 251 switches are summarized in Figure 4.

252 4 Slicing the Sandwich Attack

253 In the context of the sandwich attack, the cipher E is conceptualized as the com-
 254 position of three subciphers: E_0 , E_m , and E_1 , represented as $E = E_0 \circ E_m \circ E_1$.
 255 The intermediary component E_m is utilized to incorporate a small number of
 256 rounds via various switch techniques, directly enhancing the probability of the
 257 boomerang distinguisher. For ciphers based on **Sbox**, when only ladder switches
 258 occur in E_m , the value of r becomes 1. Consequently, the distinguishing prob-
 259 ability simplifies to $p^2 \cdot q^2 \cdot r = p^2 \cdot q^2$. Furthermore, the **Sbox** or other new
 260 switches within E_m can also contribute to improving the value of r , although
 261 not significantly compared to the ladder switch. Thus, for the sandwich attack
 262 (as illustrated in Figure 2), constructing single or very few rounds of E_m using
 263 **Sbox** or other new switches is relatively straightforward. However, employing
 264 switch techniques for a large number of rounds in E_m can introduce compat-
 265 ibility challenges. To address this, several systematic techniques [21,23,14] are
 266 introduced to effectively resolve these incompatibility issues as the number of
 267 rounds increases.

¹ This sub-case of the Trail Switch category covers all switches except TRIVIAL, LADDER, and AND when we require two opposite plane differences to be equal (refer to Table 4). The remaining sub-cases within the Trail Switch category occur when no specific conditions are imposed on opposite plane differences.

Δ_1	Δ_2	∇_1	∇_2	Switch	$Pr[\Delta_3 = \Delta_4, \nabla_3 = \nabla_4]$
0	0	0	0	-	1
0	0	0	1	LADDER	1
0	0	1	0	LADDER	1
0	0	1	1	LADDER	1
0	1	0	0	LADDER	1
0	1	0	1	AND	1
0	1	1	0	TRAIL	0
0	1	1	1	TRAIL	0
1	0	0	0	LADDER	1
1	0	0	1	TRAIL	0
1	0	1	0	AND	1
1	0	1	1	TRAIL	0
1	1	0	0	LADDER	1
1	1	0	1	TRAIL	0
1	1	1	0	TRAIL	0
1	1	1	1	AND	1

Table 4: Different Switching Probabilities to Maintain Equal Plane Differences in E_m .

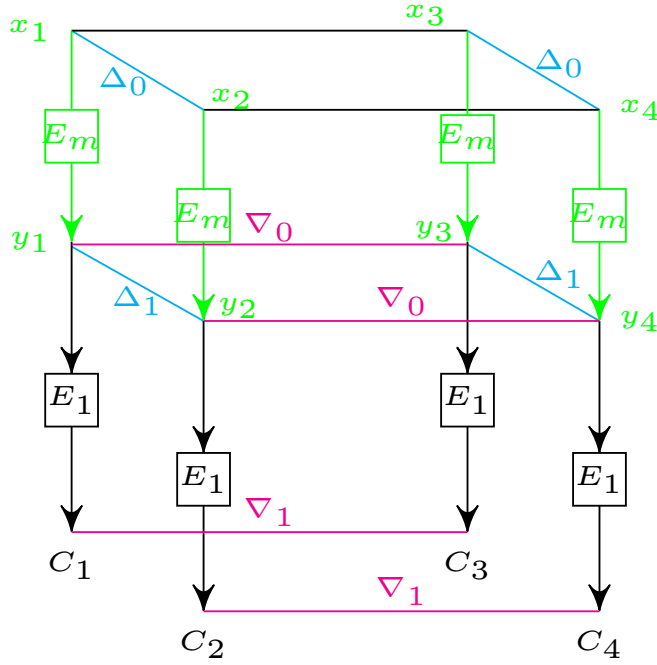


Fig. 4: Open-Sandwich Attack

268 For NLFSR-based block ciphers, it is important to highlight that only ladder
 269 or And switches have the potential to enhance the value of r in E_m and simulta-
 270 neously maintain equality in their opposite plane (state) differences. In contrast,
 271 other switch cases result in unequal opposite plane differences. While employing
 272 other switch techniques might allow the attacker to obtain the input difference
 273 Δ_0 through boomerang-style attacks, the resulting distinguishing probability is
 274 notably lower compared to the scenarios where only ladder or And switches are
 275 used.

276 In this study, our primary focus is to delve into the discussion of boomerang
 277 attacks exclusively through the utilization of ladder or And switches. Within
 278 the scope of this work, we particularly concentrate on exploring and analyzing
 279 these switches. It is worth noting that in the pursuit of identifying the optimal
 280 boomerang for NLFSR-based block ciphers, a useful approach is to conceptualize
 281 the cipher E as the composition of E_m and E_1 , expressed as $E = E_m \circ E_1$.
 282 This framework essentially constitutes a special case of a sandwich attack, with
 283 E_0 being omitted. We refer to this technique as the “open-face sandwich at-
 284 tack”. The distinguishing probability of this attack will be $r \cdot q^2$. This attack is
 285 demonstrated in Figure 4.

286 4.1 Our Observations

287 Consider a straightforward boomerang structure $E = E_0 \circ E_1$ (as depicted in
 288 Figure 1), which corresponds to optimal differentials $\Delta_0 \rightarrow \Delta_1$ of E_0 with a
 289 probability of p , and $\nabla_0 \rightarrow \nabla_1$ of E_1 with a probability of q . In this context,
 290 the probability of success for this boomerang distinguisher can be approximately
 291 evaluated using the formula $p^2 \cdot q^2$. Now, for the simple boomerang within NLFSR-
 292 based block ciphers, let p represent the count of active AND gates for the differ-
 293 ential $\Delta_0 \rightarrow \Delta_1$ in one of the two opposing upper planes within E_0 . Likewise,
 294 let q denote the count of active AND gates for the differential $\nabla_0 \rightarrow \nabla_1$ in one
 295 of the two opposing lower planes within E_1 . However, it is important to note
 296 that in this scenario, the actual probability of satisfying this boomerang tends
 297 to be notably higher than the theoretical probability $p^2 \cdot q^2$. This discrepancy
 298 between theoretical and actual probabilities sparked our curiosity to further ex-
 299 plore the behavior of such boomerang attacks within NLFSR-based ciphers and
 300 to accurately estimate the theoretical probability.

301 In NLFSR-based block ciphers, AND gates constitute the sole non-linear op-
 302 erations utilized within the cipher structure. When examining a boomerang sce-
 303 nario (as illustrated in Figure 4), consider the differential $\Delta_0 \rightarrow \Delta_1$ pertaining
 304 to E_m and the differential $\nabla_0 \rightarrow \nabla_1$ associated with E_1 . Within the boomerang
 305 quartet, the plane differences in each round align with the category of distinct
 306 switches mentioned earlier.

307 Boomerangs involving trail switches cause the opposite plane differences to
 308 become unequal, simultaneously compelling the increase of trail switches across
 309 rounds. Consequently, these trail switch-based boomerangs lead to a significant
 310 reduction in the overall probability. As a result, the quest for an improved
 311 boomerang distinguisher involves seeking a promising differential boomerang

312 path that traverses through various switches while excluding the other switches.
313 Upon discovering such an optimal boomerang path, characterized by the right
314 number of ladder or And switches, the probability can be precisely computed
315 using the formula $r \cdot q^2$.

316 4.2 Searching of Good Boomerang Trails

317 In our pursuit of identifying effective boomerang trails for the cipher, our strat-
318 egy revolves around optimizing the number of ladder or And switches necessary
319 to create a boomerang effect. To accomplish this, we have developed a straight-
320 forward model that employs mixed-integer linear programming (MILP) to search
321 for the optimal boomerang trails.

322 In this MILP model, a pragmatic approach is taken: we maintain four state
323 differences and focus on optimizing the plane differences by assigning appropriate
324 weights to the ladder or And switches. Specifically, when dealing with rounds of
325 E_m , we assign a weight of 1 to the ladder or And switches. Conversely, for the
326 lower part (E_1), we assign a weight of 2 to the ladder or And switches. Within
327 the framework of the optimal boomerang trail, let us denote w_1 and w_2 as the
328 cumulative weights of E_m and E_1 , respectively. Consequently, the probability
329 associated with the boomerang trail can be expressed as $r \cdot q^2 = 2^{-w_1-w_2}$. This
330 formulation allows us to effectively determine and optimize the probability of
331 the boomerang trail.

332 It is important to note that this probability accurately represents the boomerang's
333 success when both differences Δ_1 and ∇_1 are predetermined. However, if Δ_1 and
334 ∇_1 are arbitrary differences, the calculated probability can potentially experi-
335 ence a notable enhancement due to the existence of multiple paths within the
336 boomerang or due to the inclusion of trail switches. In such scenarios, the actual
337 probability of obtaining a right boomerang quartet could be higher than the
338 calculated value due to the increased flexibility introduced by these variations.

339 5 Attacks on TinyJambu

340 The TinyJambu [25] is an authentication scheme that is chosen as one of the fi-
341 nalists in the NIST lightweight cryptography (LWC) competition. It employs an
342 NLFSR-based keyed permutation as its internal structure, without a key sched-
343 ule function. TinyJambu provides three versions with key sizes of 128, 192, and
344 256 bits respectively. During initialization, the initial version of TinyJambu [24]
345 utilizes 384 rounds to process the nonce and associated data, while for process-
346 ing the message, it employs 1024/1152/1280 rounds depending on the key size
347 of 128/192/256 bits. However, in 2020, Saha et al. [19] demonstrated a forgery
348 attack on the full-round TinyJambu scheme with a probability close to $2^{-70.64}$,
349 indicating a security level near 64 bits. In response, the designers increased the
350 number of rounds from 384 to 640 to enhance the scheme's security. For a more
351 comprehensive understanding of TinyJambu's specifications, please refer to [25].
352 Regarding the keyed permutation of TinyJambu in the secret key setting, further

353 research has revealed certain vulnerabilities. In the work [20], key-recovery at-
 354 tacks on all variant sizes were presented, achieving results close to the birthday
 355 bound of 2^{64} .

356 Dunkelman et al. [10] demonstrated a zero-sum distinguisher for 544 rounds
 357 out of the 1024-round TinyJambu keyed permutation, achieving this with a com-
 358 plexity of 2^{23} . Furthermore, in their work [11], the authors revealed related-key
 359 forgery attacks targeting various TinyJambu variants. These attacks exhibited
 360 differential probabilities of 2^{-16} , 2^{-12} and 2^{-10} for 128, 192, and 256-bit keys,
 361 respectively, emphasizing potential security concerns.

362 In another development, Jana et al. [16] identified a full-round differen-
 363 tial trail within the 1024-round TinyJambu keyed permutation. This trail dis-
 364 played an exceptionally low probability of 2^{-108} , revealing non-random prop-
 365 erties within the keyed permutation. Additionally, in this attack, the authors
 366 demonstrated improved related-key differential probabilities of 2^{-14} , 2^{-10} and
 367 2^{-8} for 128, 192, and 256-bit keys, respectively, highlighting potential vulnera-
 368 bilities in TinyJambu’s security characteristics.

369 In this section, our focus is on the TinyJambu keyed permutation, where we
 370 investigate the application of different switch techniques to explore boomerang
 371 properties. By employing these techniques, we achieve significant advancements
 372 in the analysis of TinyJambu with 640 rounds in the secret-key settings, surpass-
 373 ing the success rates of previous attacks. Furthermore, we present the related-key
 374 boomerang attacks for all the TinyJambu variants.

375 5.1 Specification

376 TinyJambu is an authenticated encryption with associated data (AEAD) scheme,
 377 featuring a 128-bit non-linear feedback shift register (NLFSR)-based keyed per-
 378 mutation with a 128-bit state size and 32-bit message block size. It was se-
 379 lected as one of the top ten finalists in the NIST Lightweight Cryptography
 380 (LWC) competition, competing among 56 submissions. The 128-bit keyed per-
 381 mutation, represented as P_l^K , comprises l rounds, with the secret key K be-
 382 longing to $\mathbb{F}_2^{|K|}$, where K is defined as $(k_{|K|-1}, k_{|K|-2}, \dots, k_1, k_0)$. This per-
 383 mutation offers support for three key sizes: 128 bits, 192 bits, and 256 bits.
 384 In this work, we denote an l -round keyed permutation of TinyJambu as \mathcal{P}_l .
 385 Each round of the permutation, $P_l^K : \mathbb{F}_2^{128} \rightarrow \mathbb{F}_2^{128}$, transforms an initial state
 386 $(s_{127}, s_{126}, \dots, s_1, s_0)$ into a final state $(s_f, s_{127}, s_{126}, \dots, s_2, s_1)$, where s_f is
 387 calculated as $s_0 \oplus s_{47} \oplus \overline{s_{70} s_{85}} \oplus s_{91} \oplus k_{i \bmod |K|}$. Figure 5 refers to a visual
 388 representation of this permutation.

389 TinyJambu offers three variants, denoted as TinyJambu-128, TinyJambu-192,
 390 and TinyJambu-256, each defined by specific parameters listed in Table 5. The
 391 encryption process in TinyJambu involves four main phases: Initialization, Asso-
 392 ciated Data Processing, Encryption, and Finalization. We refer to Figure 6 for
 393 an overview of the TinyJambu mode’s overall structure. Detailed specifications
 394 for the permutations P_l and \hat{P}_l can be found in Table 5. The complete details of
 395 this scheme can be found in [25].

414 Jambu cipher as $E_m \circ E_1$, with a focus on minimizing the ladder/And switches
 415 to create a potent boomerang distinguisher that is both efficient and effective.

Table 6: Boomerang Distinguishers of TinyJambu through MILP Search

Rounds	Ladder Switch	And Switch	Distinguishing Probability	Input Difference (Upper Plane)				Output Difference (Lower Plane)				Success Probability
				Δ_0	Δ_1	∇_0	∇_1					
320	6	0	2^{-9}	$\Delta_0 = 0x00000120$	00000000	02000000	00000400	$\nabla_0 = 0x00000001$	20000000	00020000	00000004	99.9%
	7	0	2^{-10}	$\Delta_0 = 0x00000400$	00000000	80000000	00000000	$\nabla_0 = 0x00000001$	20000000	00020000	00000004	99.9%
384	8	0	2^{-12}	$\Delta_0 = 0x00000241$	00020000	04000000	00000800	$\nabla_0 = 0x00020010$	00000004	80000000	00080000	99.9%
	4	4	2^{-12}	$\Delta_0 = 0x00020010$	00000004	80000000	00080000	$\nabla_0 = 0x00200100$	00000048	00000000	00800000	100%
640 ¹	24	2	2^{-39}	$\Delta_0 = 0x00001000$	80000000	24000000	00004000	$\nabla_0 = 0x00008004$	00000001	20000000	00020000	-

Table 7: Amplified Boomerang Distinguishers of TinyJambu

Rounds	Distinguishing Probability	Input Difference (Upper Plane)				Output Difference (Lower Plane)				Success Probability
		Δ_0	Δ_1	∇_0	∇_1					
288	1	$\Delta_0 = 0x00004000$	00000000	80000000	00000000	$\nabla_0 = 0x00000000$	00000000	00000400	00000020	100%
320	1	$\Delta_0 = 0x00001000$	00000000	20000000	00000000	$\nabla_0 = 0x00000000$	00000000	00000040	00000002	100%
		$\Delta_0 = 0x00004000$	00000000	80000000	00000000	$\nabla_0 = 0x00000000$	00000000	00000004	00000000	100%
384	2^{-4}	$\Delta_0 = 0x00000120$	00000000	02000000	00000400	$\nabla_0 = 0x00000000$	00000000	00000004	00000000	99.8%
	2^{-4}	$\Delta_0 = 0x00000241$	00020000	04000000	00000800	$\nabla_0 = 0x00000000$	00000000	00000010	00000000	98%
640	2^{-22}	$\Delta_0 = 0x00048200$	04000008	00000000	00100000	$\nabla_0 = 0x00000000$	00000000	20000000	01000000	95%
	2^{-24}	$\Delta_0 = 0x00001000$	80000000	24000000	00004000	$\nabla_0 = 0x20000000$	01020000	00080004	00004081	95%

416 5.3 Results on TinyJambu

417 **Single-key Boomerang Attacks** By employing our proposed MILP modeling,
 418 we have successfully identified a boomerang distinguisher for TinyJambu span-
 419 ning up to 320 rounds. Our optimal solution involves 6 ladder switches occurring
 420 at specific rounds: 0, 32, 47, 168, 200, and 215. Additionally, the second best so-
 421 lution consists of 7 ladder switches at rounds 107, 122, 144, 159, 168, 200, and
 422 215. These boomerang trails are detailed in Table 6.

² Sub-optimal solution due to MILP solver limitations.

423 Our search approach treats E as two equal subciphers: E_m and E_1 . For the
 424 optimal solution, we find three ladder switches in each of E_m and E_1 . This
 425 results in $r = 2^{-3}$ and $q = 2^{-3}$, yielding a distinguishing probability of $r \cdot q^2 =$
 426 2^{-9} . Similarly, for the second best solution, we have $r = 2^{-4}$, $q = 2^{-3}$, and a
 427 probability of 2^{-10} .

428 Alternatively, if we consider the boomerang trail as two distinct differentials
 429 of 160 rounds each, denoted as $E = E_0 \circ E_1$, the distinguishing probability
 430 becomes $p^2 \cdot q^2$, where $p = \Pr(\Delta_0 \rightarrow \Delta_1)$ and $q = \Pr(\nabla_0 \rightarrow \nabla_1)$. For the first
 431 320-round boomerang distinguisher in Table 6, we have $p = 2^{-3}$ and $q = 2^{-3}$,
 432 resulting in a probability of 2^{-12} . Similarly, for the second distinguisher of 320
 433 rounds, with $p = 2^{-4}$ and $q = 2^{-3}$, the probability is 2^{-14} .

434 In our comprehensive investigation, we have delved into the intricacies of
 435 boomerang paths, particularly focusing on larger rounds, namely 384 rounds
 436 and 640 rounds. For the 384-round scenario, our diligent analysis led to the dis-
 437 covery of an optimal boomerang path, meticulously comprising 8 ladder switches
 438 strategically activated at specific rounds: 31, 46, 159, 174, 215, 230, 262, and 277.
 439 When considering fixed values for Δ_1 and ∇_0 , this carefully designed boomerang
 440 path yields a probability for the boomerang distinguisher, precisely calculated as
 441 $r \cdot q^2 = 2^{-4} \cdot 2^{-8} = 2^{-12}$. This finding underscores that even with a substantial
 442 number of cipher rounds, the likelihood of success for this boomerang attack
 443 remains relatively low.

444 In a more extensive scenario involving 640 rounds, our investigation led to
 445 the identification of an intricate boomerang trail. This path involves the acti-
 446 vation of 26 ladder/And switches, consisting of 24 ladder switches and 2 And
 447 switches, thoughtfully positioned throughout the rounds. The resulting distin-
 448 guishing probability for this extensive boomerang path is significantly lower,
 449 quantified as 2^{-41} . This difference emphasizes the escalating difficulty and dimin-
 450 ishing success rate associated with boomerang attacks as the number of rounds
 451 in the cipher increases. Our approach to identifying these optimal boomerang
 452 trails through various switches effectively captures the probability distribution,
 453 shedding light on the challenging landscape of NLFSR-based cryptographic ci-
 454 pher analysis.

455 Moreover, we have explored the concept of amplified boomerangs in this
 456 context to enhance the overall probability of boomerang distinguishers. Our ap-
 457 proach involves deliberately seeking suboptimal solutions from our MILP search.
 458 The goal is to create a boomerang with the input difference Δ_0 and the output
 459 difference ∇_1 that possesses numerous alternate paths. This strategic manipu-
 460 lation has led to notably improved probabilities for these rounds of TinyJambu,
 461 which are detailed in Table 7.

462 **Related-key Boomerang Attacks** In a similar manner, we applied the MILP
 463 model to investigate related-key boomerang trails for the TinyJambu-128 cipher.
 464 For a 384-round cipher, we identified an optimal solution that resulted in a
 465 deterministic boomerang trail, requiring no ladder or And switches.

Table 8: Related-key Boomerang Distinguishers of TinyJambu Variants through MILP Search

Variant	Rounds	Ladder Switch	And Switch	Distinguishing Probability	Upper Trail Difference	Lower Trail Difference	Upper Key Difference	Lower Key Difference	Success Probability
TinyJambu128	384	0	0	1	$\Delta_0 = 0x00102400$ 00000020 40000000 00000000 $\Delta_1 = 0x00000000$ 00000000 00000400 00000000	$\nabla_0 = 0x00000008$ 00000000 00100000 00000000 $\nabla_1 = 0x00000000$ 00000000 00002200 00000010	0x00000400 00000020 40000000 00000000 0x04000000 00000000 00002000 00000000	0x00000000 00000000 00000000 00000000 0x00000000 00000000 00000000 00000000	100%
	512 ¹	4	0	2 ⁻⁶	$\Delta_0 = 0x00090000$ 00000010 00000000 00200000 $\Delta_1 = 0x00000000$ 00000000 00000000 00200000	$\nabla_0 = 0x00000008$ 00000000 00100000 00000000 $\nabla_1 = 0x00000000$ 00000000 00100000 00000000	0x00000000 00000000 00000000 00200000 0x00000000 00000000 00100000 00000000	0x00000000 00000000 00000000 00000000 0x20000000 00000000 00002000 00000000	92%
	640 ²	5	0	2 ⁻⁷	$\Delta_0 = 0x40000000$ 12000000 00002000 00000000 $\Delta_1 = 0x00000000$ 00000000 00000000 02000000	$\nabla_0 = 0x00001200$ 00000000 20000000 00000000 $\nabla_1 = 0x00000000$ 00000000 00002000 00000010	0x40000000 02000000 00002000 00000000 0x20000000 00004000 00002000 00000000	0x00000000 04000000 00000000 00000040 0x00000000 04000000 00000000 00000040	22%
TinyJambu192	1024 ¹	16	0	2 ⁻²⁴	$\Delta_0 = 0x00000000$ 00000000 00000000 00000000 $\Delta_1 = 0x00000000$ 00000000 00000000 00000000	$\nabla_0 = 0x00000000$ 00000000 00000000 00000000 $\nabla_1 = 0x00000000$ 00000000 00000000 00000000	0x00000000 04000000 00000000 00000040 0x00000000 04000000 00000000 00000040	0x00000000 04000000 00000000 00000040 0x00000000 04000000 00000000 00000040	100%
	512	0	0	1	$\Delta_0 = 0x4002201$ 80008120 4c000000 00000000 $\Delta_1 = 0x00000000$ 00000000 00000000 00000000	$\nabla_0 = 0x00000000$ 00000000 00000000 00000000 $\nabla_1 = 0x00000000$ 00000000 00000000 00000000	0x00000401 80008120 4c000000 00000000 0x00000000 00000000 00000000 00000000	0x00000000 00000000 00000000 00000000 0x00000000 00000000 00000000 00000000	100%
	640 ¹	4	0	2 ⁻⁶	$\Delta_0 = 0x00000000$ 00000000 00000000 00000000 $\Delta_1 = 0x12000000$ 00002000 00000000 40000000	$\nabla_0 = 0x00000000$ 00000000 00000000 00000000 $\nabla_1 = 0x00000000$ 00002000 00000000 00000000	0x00000000 00000000 00000000 40000000 0x00000000 00000000 00000000 00000000	0x00000000 00000000 00000000 00000000 0x00000000 00000000 00000000 00000000	72%
TinyJambu256	1152 ¹	12	0	2 ⁻¹⁸	$\Delta_0 = 0x00000000$ 00000000 00000000 00000000 $\Delta_1 = 0x00000000$ 00002000 00000000 00000000	$\nabla_0 = 0x00000000$ 00002000 00000000 00000000 $\nabla_1 = 0x00000000$ 00002000 00000000 00000000	0x00000000 00002000 00000000 00000000 0x01000000 00002000 00000000 00000000	0x00000000 00002000 00000000 00000000 0x01000000 00002000 00000000 00000000	84%
	640	0	0	1	$\Delta_0 = 0x40180400$ 22008030 08000000 00000000 $\Delta_1 = 0x00000000$ 00000000 00000000 22008030	$\nabla_0 = 0x00104004$ 26c00020 80000000 00000000 $\nabla_1 = 0x00000000$ 00000000 00000000 26c00020	0x00000000 22008030 08000000 00000000 0x00000000 00000000 00000000 26c00020	0x00000000 22008030 08000000 00000000 0x00000000 00000000 00000000 26c00020	100%
	1280 ¹	8	0	2 ⁻¹²	$\Delta_0 = 0x00000000$ 00000000 40000000 00000000 $\Delta_1 = 0x00000000$ 00000000 00000000 00000000	$\nabla_0 = 0x01000000$ 00000000 00000000 00000000 $\nabla_1 = 0x00000000$ 00000000 00000000 00000000	0x00000000 40000000 00000000 00000000 0x01000000 00000000 00000000 00000000	0x00000000 40000000 00000000 00000000 0x01000000 00000000 00000000 00000000	91%

483 Furthermore, our exploration extended to related-key boomerang distinguishers,
484 where we successfully identified deterministic distinguishers spanning 512
485 and 640 rounds for TinyJambu-192 and TinyJambu-256, respectively. In the
486 case of full rounds for TinyJambu-192, we discovered a sub-optimal boomerang
487 path featuring twelve ladder switches, resulting in a distinguishing probability of
488 2^{-18} . Similarly, for the complete rounds of TinyJambu-1280, we encountered a
489 sub-optimal solution characterized by eight ladder switches, resulting in a prob-
490 ability of 2^{-18} .

491 We have summarized these discovered trails and their respective character-
492 istics in Table 8. Furthermore, our exploration extended to finding amplified
493 boomerang trails by considering sub-optimal solutions, thereby increasing the
494 overall probability of these distinguishers. Detailed information about these am-
495 plified boomerang trails and their success probabilities can also be found in
496 Table 9.

497 **Experimental Results** Under both single-key and related-key settings, we
498 have rigorously conducted practical verifications for all the boomerang paths
499 of TinyJambu presented in Tables 6,8. These paths were discovered using the
500 MILP (Mixed-Integer Linear Programming) search method. This meticulous val-
501 idation process ensures the reliability and practical applicability of our reported
502 boomerang paths. Furthermore, we have subjected our findings related to the
503 best amplified boomerang attacks on TinyJambu, as outlined in Tables 7,9, to
504 thorough validation across scenarios involving both single-key and related-key
505 settings. For a comprehensive understanding of our verification process, as well
506 as access to detailed results and supporting information, we refer to [1]. These
507 verifications constitute substantial evidence that our reported boomerang paths,
508 success rates, and findings have undergone rigorous real-world testing and anal-
509 ysis, affirming their reliability and practical utility.

510 6 Attacks on KATAN

511 The KATAN cipher, as described in [7], is a family of NLFSR-based block ciphers
512 with three variants corresponding to block sizes of 32, 48, and 64 bits. The
513 state of the KATAN cipher consists of two registers, namely L_1 and L_2 , which
514 have different sizes based on their state sizes. All variants of KATAN employ
515 254 rounds and use an 80-bit key to derive 508 subkey bits through a linear
516 feedback shift register (LFSR) in the key schedule function. In the round function
517 of KATAN, both registers, L_1 and L_2 , function as NLFSRs. The feedback bit of
518 L_1 is fed into the least significant bit (LSB) of L_2 , and vice versa. Additionally,
519 the state bits are shifted by one position from the least significant bit (LSB) to
520 the most significant bit (MSB) in each round. For the KATAN48 and KATAN64
521 variants, the round function is repeated 2 and 3 times respectively, using the
522 same subkeys. For more detailed information about the KATAN cipher, please
523 refer to [7].

524 In previous research, Isobe et al.[15] introduced a related-key boomerang
 525 distinguisher for KATAN32 consisting of 140 rounds, achieving a distinguisher
 526 probability of $2^{-27.2}$. Building upon their work, Chen et al.[8] further enhanced
 527 the boomerang distinguisher by employing the branch-and-bound method, re-
 528 sulting in an improved probability of $2^{-26.58}$. These advancements demonstrated
 529 the vulnerability of KATAN32 to related-key boomerang attacks.

530 In a distinct research direction, a recent work by Jana et al. [16] introduced
 531 the DEEPAND model, specifically designed for analyzing the impact of multiple
 532 AND gates within NLFSR-based ciphers like KATAN. This model capitalizes on
 533 exploiting correlations among these AND gates to enhance the probability of
 534 differential trails. Through this technique, the researchers successfully elevated
 535 the efficiency of a differential trail. Leveraging the capabilities of the DEEPAND
 536 model, the authors achieved significant advancements. They managed to iden-
 537 tify and establish highly effective differential trails, encompassing a remarkable
 538 70 rounds. This achievement resulted in the development of a notably potent
 539 related-key boomerang distinguisher. By employing this innovative approach, a
 540 deeper understanding of the cipher’s vulnerabilities was obtained, and this, in
 541 turn, facilitated the creation of more powerful and effective attack strategies.

542 6.1 Specification

543 The KATAN family is an efficient hardware-oriented block cipher, featuring three
 544 variants: KATAN32, KATAN48, and KATAN64, designed for 32-bit, 48-bit, and
 545 64-bit block sizes, respectively. All variants employ 254 rounds and utilize the
 546 non-linear functions $\mathcal{NF1}$ and $\mathcal{NF2}$. They share a common LFSR-based key
 547 schedule that takes an 80-bit key as input. The fundamental structure of the
 548 KATAN cipher involves loading plaintext into two registers, L_1 and L_2 . During
 549 each round, several bits from these registers are processed by the non-linear
 550 functions $\mathcal{NF1}$ and $\mathcal{NF2}$, and the results are loaded into the least significant
 551 bits of the registers. The key schedule function expands the 80-bit user-provided
 552 key k_i ($0 \leq i < 80$) into a 508-bit subkey sk_i ($0 \leq i < 508$) using specific linear
 553 operations.

$$sk_i = \begin{cases} k_i, & 0 \leq i < 80 \\ k_{i-80} \oplus k_{i-61} \oplus k_{i-50} \oplus k_{i-13}, & 80 \leq i < 508. \end{cases}$$

Also, the two non-linear functions are defined as follows:

$$\mathcal{NF}_1(L_1) = L_1[x_1] \oplus L_1[x_2] \oplus (L_1[x_3] \cdot L_1[x_4]) \oplus (L_1[x_5] \cdot IR) \oplus k_a$$

$$\mathcal{NF}_2(L_2) = L_2[y_1] \oplus L_2[y_2] \oplus (L_2[y_3] \cdot L_2[y_4]) \oplus (L_2[y_5] \cdot L_2[y_6]) \oplus k_b,$$

554 The KATAN cipher employs a predefined round constant known as IR (details
 555 provided in [?]), along with two subkey bits, k_a and k_b , in its operations. The
 556 selection of specific bits, denoted as x_i for $1 \leq i \leq 5$ and y_i for $1 \leq i \leq 6$,
 557 is variant-specific and outlined in Table 10. In the case of KATAN32, the i -th
 558 round function, illustrated in Figure 7, assigns k_a the value of k_{2i} and k_b the

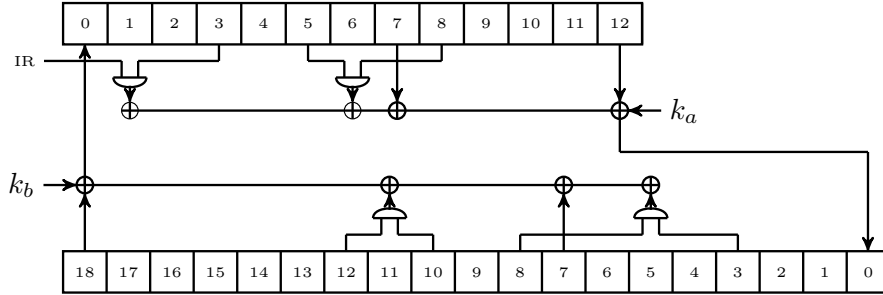


Fig. 7: Round Function of KATAN [32]

559 value of k_{2i+1} . After 254 rounds, the values contained in the registers are output
 560 as ciphertext. In KATAN48, a unique feature is the application of the non-linear
 561 functions \mathcal{NF}_1 and \mathcal{NF}_2 twice within a single round. Initially, the first pair of
 562 \mathcal{NF}_1 and \mathcal{NF}_2 is applied, and following the update of the registers, they are
 563 reapplied using the same subkeys. Likewise, in the KATAN64 variant, each round
 564 involves three consecutive applications of \mathcal{NF}_1 and \mathcal{NF}_2 with the same key bits.
 565 More details regarding the specifications of the KATAN family of ciphers can be
 566 found in [7].

Table 10: Parameters of KATAN Variants

KATAN Variants	$ L_1 $	$ L_2 $	x_1	x_2	x_3	x_4	x_5	y_1	y_2	y_3	y_4	y_5	y_6
KATAN [32]	13	19	12	7	8	5	3	18	7	12	10	8	3
KATAN [48]	19	29	18	12	15	7	6	28	19	21	13	15	6
KATAN [64]	25	39	24	15	20	11	9	38	25	33	21	14	9

567 6.2 MILP Modelling

568 In our approach to attacking KATAN, we have chosen to simplify things by
 569 narrowing our focus from four planes to just two. This decision aims to make the
 570 attack more efficient in terms of both computation and time. When it comes to
 571 using MILP modeling for attacking KATAN, we follow a straightforward strategy.
 572 We treat the KATAN cipher as if it is the middle part, denoted as E_m , in the
 573 model. The main goal is to reduce the use of ladder/And switches as much as
 574 possible. This emphasis on minimizing these specific switches helps us create
 575 a powerful boomerang distinguisher that is not only efficient but also highly
 576 effective in exploiting the cipher’s vulnerabilities.

Table 11: Related-key Boomerang Distinguishers of KATAN32 through MILP Search

Rounds	Ladder	And	Distinguishing	Upper Trail	Upper Trail	Key Difference	Key Difference	Success
	Switch	Switch	Probability	Differences	Differences	(Upper Trail)	(Lower Trail)	Probability
120	5	2	2^{-11}	$\Delta_0 = 0x00042000$ $\Delta_1 = 0x08000002$	$\nabla_0 = 0x8400c010$ $\nabla_1 = 0x01000002$	0x40110020000000000802	0x026008401808a041a660	86.6%
	5	2	2^{-11}	$\Delta_0 = 0x00004000$ $\Delta_1 = 0x00f80084$	$\nabla_0 = 0x20058400$ $\nabla_1 = 0x01000000$	0x00010044008000000200	0x241157c289ba4c354b3b	86.5%
140 ¹	14	0	2^{-21}	$\Delta_0 = 0x00062000$ $\Delta_1 = 0x00400801$	$\nabla_0 = 0xa4024010$ $\nabla_1 = 0x00b80084$	0x4051 00200000 0000080a	0x63c4 cf451630 862a0c25	97%
	10	4	2^{-21}	$\Delta_0 = 0x80031000$ $\Delta_1 = 0x01200400$	$\nabla_0 = 0xa4024010$ $\nabla_1 = 0x00b80084$	0x0140 00800000 00002029	0x63c4 cf451630 762a0c25	25%

577 **6.3 Results on KATAN**

578 **Related-key Boomerang Attacks** Through the application of our MILP
579 model to KATAN32, we have successfully uncovered a related-key boomerang
580 distinguisher spanning up to 120 rounds. Our optimal solution entails the acti-
581 vation of two And switches at positions 32 and 35, as well as five ladder switches
582 at positions 57, 61, 64, 66, and 68. Additionally, we have identified another op-
583 timal solution with the same configuration: two And switches at positions 95
584 and 98, and five ladder switches at positions 25, 28, 56, 60, and 62. Notably, in
585 both cases, three switches are engaged in the first 60 rounds, while four switches
586 are triggered in the subsequent 60 rounds. Consequently, the probability of the
587 boomerang distinguisher is determined to be $r \cdot q^2 = 2^{-3} \cdot 2^{-8} = 2^{-11}$.

588 In our pursuit of effective boomerang trails spanning 140 rounds, we have
589 uncovered multiple optimal solutions using our MILP search. Among these, one
590 solution stands out prominently. This particular solution involves the activation
591 of fourteen ladder switches at distinct positions: 32, 35, 57, 60, 62, 69, 71, 74, 76,
592 78, 105, 108, and 136. This boomerang boasts a probability of $r \cdot q^2 = 2^{-7} \cdot 2^{-14} =$
593 2^{-21} . Another noteworthy solution we have identified features four And switches
594 at positions 1, 58, 61, and 136, accompanied by ten ladder switches at positions
595 33, 36, 63, 68, 71, 74, 76, 78, 105, and 108. These intricate details of the optimal
596 boomerang trails for 140 rounds are meticulously documented in Table 11.

Table 12: Related-key Amplified Boomerang Distinguishers of KATAN32

Rounds	Distinguishing	Input Difference	Output Difference	Key Difference	Key Difference	Success
	Probability	(Upper Trail)	(Lower Trail)	(Upper Trail)	(Lower Trail)	Probability
120	2^{-7}	$\Delta_0 = 0x00042000$	$\nabla_1 = 0x01000002$	0x4011 00200000 00000802	0x0260 08401808 a041a660	64%
140	2^{-15}	$\Delta_0 = 0x00062000$	$\nabla_1 = 0x00b80084$	0x4051 00200000 0000080a	0x63c4 cf451630 862a0c25	70%

Table 13: Single-key Boomerang Distinguishers of KATAN32 through MILP Search

Rounds	Ladder Switch	And Switch	Distinguishing Probability	Upper Trail Differences	Lower Trail Differences	Success Probability
60	9	4	2^{-19}	$\Delta_0 = 0x00020040$ $\Delta_1 = 0x00100210$	$\nabla_0 = 0x0001a020$ $\nabla_1 = 0x00080108$	71%
	8	5	2^{-19}	$\Delta_0 = 0x00034040$ $\Delta_1 = 0x00100210$	$\nabla_0 = 0x00018020$ $\nabla_1 = 0x00080108$	70%
72	13	9	2^{-31}	$\Delta_0 = 0x00020040$ $\Delta_1 = 0x0420840a$	$\nabla_0 = 0x8004c600$ $\nabla_1 = 0x00080108$	--
84	14	10	2^{-34}	$\Delta_0 = 0x10042080$ $\Delta_1 = 0x00400840$	$\nabla_0 = 0x10068080$ $\nabla_1 = 0x00400840$	--

597 Our dedicated efforts are directed towards identifying efficient and potent
598 boomerang distinguishers within the domain of cryptographic ciphers. Addition-
599 ally, we have explored amplified boomerang trials through suboptimal solutions,
600 further enhancing the overall probability of these distinguishers. A compre-
601 hensive list of these trails, along with their amplified probabilities, is provided in
602 Table 12.

603 **Single-key Boomerang Attacks** In the context of single-key settings, we
604 employed an MILP model to successfully identify a boomerang distinguisher for
605 various numbers of rounds. Here are the details of our findings:

606 For a 60-round cipher, we discovered two optimal solutions for the boomerang
607 distinguisher. In the first solution, the boomerang path involved nine ladder

Table 14: Amplified Boomerang Distinguishers of KATAN32

Rounds	Distinguishing Probability	Input Difference (Upper Trail)	Output Difference (Lower Trail)	Success Probability
60	2^{-14}	$\Delta_0 = 0x00020040$	$\nabla_1 = 0x00080108$	72%
	2^{-14}	$\Delta_0 = 0x00034040$	$\nabla_1 = 0x00080108$	70%
72	2^{-24}	$\Delta_0 = 0x00020040$	$\nabla_1 = 0x00080108$	65%
84	2^{-30}	$\Delta_0 = 0x10042080$	$\nabla_1 = 0x00400840$	60%

608 switches occurring at positions 18, 21, 24, 29, 33, 35, 37, 49, and 52, along with
609 four AND switches at positions 2, 4, 6, and 55. In the second solution, the path
610 consisted of eight ladder switches at positions 18, 21, 24, 29, 33, 35, 37, and 49,
611 along with five AND switches at positions 2, 4, 6, 52, and 55. In both cases, seven
612 switches were active during the initial 60 rounds, and six switches were active
613 during the latter 60 rounds. As a result, the probability of the distinguisher was
614 computed as $r \cdot q^2 = 2^{-7} \cdot 2^{-12} = 2^{-19}$.

615 Similarly, for a 72-round cipher, we identified a boomerang path comprising
616 a total of twenty-two ladder and AND switches. Thirteen switches were active
617 during the first 36 rounds, and nine switches were active during the last 36
618 rounds. This yielded a probability of $2^{-13} \cdot 2^{-18} = 2^{-31}$ for the distinguisher's
619 success.

620 Finally, in the case of an 84-round cipher, our investigation led to the dis-
621 covery of a boomerang path involving thirty-four ladder and AND switches.
622 Fourteen switches were active during the upper 42 rounds, and ten switches
623 were active during the lower 42 rounds. Consequently, the probability of this
624 boomerang distinguisher was calculated as $2^{-14} \cdot 2^{-20} = 2^{-34}$.

625 We also delved into the exploration of amplified boomerang trails through
626 optimal solutions to enhance the overall probability of these distinguishers. The
627 details of these trails and their amplified probabilities are given in Table 14.

628 **Experimental Results** We have meticulously conducted practical validations
629 for all the boomerang paths associated with KATAN32, as presented in Tables 13
630 and 11. These paths were discovered using the MILP (Mixed-Integer Linear Pro-
631 gramming) search method, and we rigorously assessed their validity under both
632 single-key and related-key settings. This comprehensive validation process en-
633 sures the dependability and practical applicability of the reported boomerang
634 paths. Furthermore, our investigations into the best amplified boomerang attacks
635 on KATAN32, which are detailed in Tables 14 and 12, have undergone extensive
636 verification across various scenarios, encompassing both single-key and related-
637 key settings. For a more comprehensive understanding of our validation process,
638 detailed results, and supporting information, we refer to [1]. These rigorous val-
639 idations provide robust evidence that our reported boomerang paths, success
640 rates, and discoveries have been subjected to stringent real-world testing and
641 analysis, affirming their practical relevance and reliability.

642 7 Discussion

643 The findings presented in this work represent a significant leap forward in the
644 field of cryptanalysis, specifically in the domain of boomerang attacks on non-
645 linear feedback shift register (NLFSR)-based block ciphers such as TinyJambu and
646 KATAN32. The successful identification of enhanced boomerang distinguishers
647 through our proposed methodology underscores its effectiveness. This discussion
648 will delve into the implications of these discoveries, their broader relevance within
649 the cryptographic landscape, and potential areas for future research.

650 Our approach employs a two-plane method in the Mixed Integer Linear Pro-
651 gramming (MILP) search, a strategy aimed at optimizing efficiency and expand-
652 ing the scope of coverage across rounds. However, it is worth noting that in
653 certain instances, the success rate of the boomerang path identified through
654 the MILP search may be relatively low. One possible reason behind this phe-
655 nomenon is that, for the upper part (i.e., the E_m part) of the cipher, a ladder
656 or And switch at a specific round may transform into Trail switch due to the
657 differential propagation through the lower part (E_1). To present a more accu-
658 rate model, assumptions considering equal differences in the opposite planes can
659 be relaxed which can leverage on the Trail switches. This presents an intrigu-
660 ing open problem: how can constraints be integrated into the MILP model to
661 effectively bypass these paths and discover the optimal boomerang path? Ad-
662 ditionally, there is room for improving the MILP model’s efficiency to facilitate
663 the exploration of a larger number of rounds.

664 Another avenue for future research lies in the exploration of unequal round
665 allocations between E_m and E_1 . Currently, our approach assumes an equal num-
666 ber of rounds for both components. Investigating whether an uneven distribution
667 of rounds can lead to the discovery of superior boomerang paths is an intriguing
668 question that merits further investigation.

669 The practical implications of the improved boomerang distinguishers are sub-
670 stantial. They empower cryptanalysts with more potent tools to assess the secu-
671 rity of cryptographic algorithms, potentially revealing vulnerabilities that may
672 have remained hidden using conventional boomerang methods. Addressing the
673 challenge of the vast number of variables in the MILP approach, we intend to
674 explore the utilization of four planes within the MILP to refine the search for
675 optimal boomerang paths through various switches, including other switches.
676 Additionally, our future work will focus on systematically calculating the overall
677 probability for amplified boomerangs, further enhancing our ability to analyze
678 and assess the security of cryptographic systems.

679 Finally, this research demonstrates the evolving landscape of cryptanalysis
680 and underscores the need for continued innovation in the quest for robust cryp-
681 tographic solutions. The challenges identified here offer exciting opportunities
682 for future investigations, ultimately contributing to the advancement of crypto-
683 graphic theory and practice.

684 8 Conclusion

685 To sum up, our study focused on a technique called boomerang attacks, which
686 are used to break block ciphers. Specifically, we were interested in ciphers that
687 use a particular structure known as NLFSR. We investigated different ways to
688 make these attacks more effective, with a special focus on a type of operation
689 called ladder or And switches.

690 In our exploration, we made an interesting discovery. The usual method to
691 calculate the likelihood of success in these attacks might not always give us the
692 right answer. We came up with a new way to estimate this probability, which

693 turned out to be different from what was commonly thought. This finding has
694 implications for how well these attacks can work in practice.

695 We then introduced a new approach to these attacks. We concentrated on
696 using ladder or And switches exclusively. This approach is somewhat similar to
697 crafting a unique type of sandwich attack. By doing this, we were able to uncover
698 vulnerabilities in NLFSR-based ciphers like TinyJambu and KATAN32.

699 In conclusion, Our study does not just provide new insights into these boomerang
700 attacks; it equips experts with improved strategies for making attacks more suc-
701 cessful. In the future, these findings will play a vital role in enhancing the security
702 of NLFSR-based block ciphers.

703 References

- 704 1. Boomerang Verification of TinyJambu and KATAN32. <https://drive.google.com/drive/u/4/folders/1l6VlrcZdIchHpPmh3vdVkhTcaBzI0gCK?hl=en>
- 705 2. National Institute of Standards and Technology (NIST): Lightweight cryp-
706 tography standardization process (2019). [https://csrc.nist.gov/projects/](https://csrc.nist.gov/projects/lightweight-cryptography)
707 [lightweight-cryptography](https://csrc.nist.gov/projects/lightweight-cryptography)
- 708 3. Biham, E., Dunkelman, O., Keller, N.: The rectangle attack - rectangling the
709 serpent. In: Pfitzmann, B. (ed.) Advances in Cryptology - EUROCRYPT 2001,
710 International Conference on the Theory and Application of Cryptographic Tech-
711 niques, Innsbruck, Austria, May 6-10, 2001, Proceeding. Lecture Notes in Com-
712 puter Science, vol. 2045, pp. 340–357. Springer (2001). [https://doi.org/10.1007/3-](https://doi.org/10.1007/3-540-44987-6_21)
713 [540-44987-6_21](https://doi.org/10.1007/3-540-44987-6_21), [https://doi.org/10.1007/3-](https://doi.org/10.1007/3-540-44987-6_21)
714 [540-44987-6_21](https://doi.org/10.1007/3-540-44987-6_21)
- 715 4. Biham, E., Shamir, A.: Differential Cryptanalysis of the Data Encryption Stan-
716 dard. Springer (1993). <https://doi.org/10.1007/978-1-4613-9314-6>, [https://doi.](https://doi.org/10.1007/978-1-4613-9314-6)
717 [org/10.1007/978-1-4613-9314-6](https://doi.org/10.1007/978-1-4613-9314-6)
- 718 5. Biryukov, A., Cannière, C.D., Dellkrantz, G.: Cryptanalysis of SAFER++. In:
719 Boneh, D. (ed.) Advances in Cryptology - CRYPTO 2003, 23rd Annual Inter-
720 national Cryptology Conference, Santa Barbara, California, USA, August
721 17-21, 2003, Proceedings. Lecture Notes in Computer Science, vol. 2729, pp.
722 195–211. Springer (2003). https://doi.org/10.1007/978-3-540-45146-4_12, https://doi.org/10.1007/978-3-540-45146-4_12
- 723 6. Biryukov, A., Khovratovich, D.: Related-key cryptanalysis of the full AES-192
724 and AES-256. In: Matsui, M. (ed.) Advances in Cryptology - ASIACRYPT
725 2009, 15th International Conference on the Theory and Application of Crypt-
726 tology and Information Security, Tokyo, Japan, December 6-10, 2009. Pro-
727 ceedings. Lecture Notes in Computer Science, vol. 5912, pp. 1–18. Springer
728 (2009). https://doi.org/10.1007/978-3-642-10366-7_1, [https://doi.org/10.1007/](https://doi.org/10.1007/978-3-642-10366-7_1)
729 [978-3-642-10366-7_1](https://doi.org/10.1007/978-3-642-10366-7_1)
- 730 7. Cannière, C.D., Dunkelman, O., Knezevic, M.: KATAN and KTANTAN -
731 A family of small and efficient hardware-oriented block ciphers. In: Clavier,
732 C., Gaj, K. (eds.) Cryptographic Hardware and Embedded Systems - CHES
733 2009, 11th International Workshop, Lausanne, Switzerland, September 6-9,
734 2009, Proceedings. Lecture Notes in Computer Science, vol. 5747, pp. 272–
735 288. Springer (2009). https://doi.org/10.1007/978-3-642-04138-9_20, [https://](https://doi.org/10.1007/978-3-642-04138-9_20)
736 doi.org/10.1007/978-3-642-04138-9_20
- 737

- 738 8. Chen, J., Teh, J., Su, C., Samsudin, A., Fang, J.: Improved (related-key) at-
739 tacks on round-reduced KATAN-32/48/64 based on the extended boomerang
740 framework. In: Liu, J.K., Steinfeld, R. (eds.) Information Security and Privacy
741 - 21st Australasian Conference, ACISP 2016, Melbourne, VIC, Australia, July 4-
742 6, 2016, Proceedings, Part II. Lecture Notes in Computer Science, vol. 9723, pp.
743 333–346. Springer (2016). https://doi.org/10.1007/978-3-319-40367-0_21, https://doi.org/10.1007/978-3-319-40367-0_21
- 745 9. Cid, C., Huang, T., Peyrin, T., Sasaki, Y., Song, L.: Boomerang connectivity ta-
746 ble: A new cryptanalysis tool. In: Nielsen, J.B., Rijmen, V. (eds.) Advances in
747 Cryptology - EUROCRYPT 2018 - 37th Annual International Conference on the
748 Theory and Applications of Cryptographic Techniques, Tel Aviv, Israel, April
749 29 - May 3, 2018 Proceedings, Part II. Lecture Notes in Computer Science,
750 vol. 10821, pp. 683–714. Springer (2018). https://doi.org/10.1007/978-3-319-78375-8_22, https://doi.org/10.1007/978-3-319-78375-8_22
- 752 10. Dunkelman, O., Ghosh, S., Lambooj, E.: Full round zero-sum distinguishers on
753 tinyjambu-128 and tinyjambu-192 keyed-permutation in the known-key setting.
754 In: Isobe, T., Sarkar, S. (eds.) Progress in Cryptology - INDOCRYPT 2022 -
755 23rd International Conference on Cryptology in India, Kolkata, India, Decem-
756 ber 11-14, 2022, Proceedings. Lecture Notes in Computer Science, vol. 13774, pp.
757 349–372. Springer (2022). https://doi.org/10.1007/978-3-031-22912-1_16, https://doi.org/10.1007/978-3-031-22912-1_16
- 759 11. Dunkelman, O., Ghosh, S., Lambooj, E.: Practical related-key forgery attacks on
760 full-round tinyjambu-192/256. IACR Trans. Symmetric Cryptol. **2023**(2), 176–
761 188 (2023). <https://doi.org/10.46586/tosc.v2023.i2.176-188>, <https://doi.org/10.46586/tosc.v2023.i2.176-188>
- 763 12. Dunkelman, O., Keller, N., Shamir, A.: A practical-time related-key attack on the
764 KASUMI cryptosystem used in GSM and 3g telephony. In: Rabin, T. (ed.) Ad-
765 vances in Cryptology - CRYPTO 2010, 30th Annual Cryptology Conference, Santa
766 Barbara, CA, USA, August 15-19, 2010. Proceedings. Lecture Notes in Computer
767 Science, vol. 6223, pp. 393–410. Springer (2010). https://doi.org/10.1007/978-3-642-14623-7_21, https://doi.org/10.1007/978-3-642-14623-7_21
- 769 13. Dunkelman, O., Keller, N., Shamir, A.: A practical-time related-key attack on
770 the KASUMI cryptosystem used in GSM and 3g telephony. J. Cryptol. **27**(4),
771 824–849 (2014). <https://doi.org/10.1007/s00145-013-9154-9>, <https://doi.org/10.1007/s00145-013-9154-9>
- 773 14. Hadipour, H., Bagheri, N., Song, L.: Improved rectangle attacks on
774 SKINNY and CRAFT. IACR Trans. Symmetric Cryptol. **2021**(2), 140–
775 198 (2021). <https://doi.org/10.46586/tosc.v2021.i2.140-198>, <https://doi.org/10.46586/tosc.v2021.i2.140-198>
- 777 15. Isobe, T., Sasaki, Y., Chen, J.: Related-key boomerang attacks on
778 KATAN32/48/64. In: Boyd, C., Simpson, L. (eds.) Information Security
779 and Privacy - 18th Australasian Conference, ACISP 2013, Brisbane, Australia,
780 July 1-3, 2013. Proceedings. Lecture Notes in Computer Science, vol. 7959,
781 pp. 268–285. Springer (2013). https://doi.org/10.1007/978-3-642-39059-3_19, https://doi.org/10.1007/978-3-642-39059-3_19
- 783 16. Jana, A., Rahman, M., Saha, D.: DEEPAND: in-depth modeling of correlated AND
784 gates for nlfsr-based lightweight block ciphers. IACR Cryptol. ePrint Arch. p. 1123
785 (2022), <https://eprint.iacr.org/2022/1123>
- 786 17. Kelsey, J., Kohno, T., Schneier, B.: Amplified boomerang attacks against reduced-
787 round MARS and serpent. In: Schneier, B. (ed.) Fast Software Encryption,

- 788 7th International Workshop, FSE 2000, New York, NY, USA, April 10-12,
789 2000, Proceedings. Lecture Notes in Computer Science, vol. 1978, pp. 75–93.
790 Springer (2000). https://doi.org/10.1007/3-540-44706-7_6, [https://doi.org/10.](https://doi.org/10.1007/3-540-44706-7_6)
791 [1007/3-540-44706-7_6](https://doi.org/10.1007/3-540-44706-7_6)
- 792 18. Murphy, S.: The return of the cryptographic boomerang. *IEEE Trans. Inf. The-*
793 *ory* **57**(4), 2517–2521 (2011). <https://doi.org/10.1109/TIT.2011.2111091>, <https://doi.org/10.1109/TIT.2011.2111091>
794 [//doi.org/10.1109/TIT.2011.2111091](https://doi.org/10.1109/TIT.2011.2111091)
- 795 19. Saha, D., Sasaki, Y., Shi, D., Sibleyras, F., Sun, S., Zhang, Y.: On the
796 security margin of tinyjambu with refined differential and linear crypt-
797 analysis. *IACR Trans. Symmetric Cryptol.* **2020**(3), 152–174 (2020).
798 <https://doi.org/10.13154/tosc.v2020.i3.152-174>, [https://doi.org/10.13154/](https://doi.org/10.13154/tosc.v2020.i3.152-174)
799 [tosc.v2020.i3.152-174](https://doi.org/10.13154/tosc.v2020.i3.152-174)
- 800 20. Sibleyras, F., Sasaki, Y., Todo, Y., Hosoyamada, A., Yasuda, K.: Birthday-
801 bound slide attacks on tinyjambu’s keyed-permutations for all key sizes. In:
802 Cheng, C., Akiyama, M. (eds.) *Advances in Information and Computer Security*
803 *- 17th International Workshop on Security, IWSEC 2022, Tokyo, Japan, August*
804 *31 - September 2, 2022, Proceedings. Lecture Notes in Computer Science, vol.*
805 *13504, pp. 107–127. Springer (2022).* https://doi.org/10.1007/978-3-031-15255-9_6,
806 https://doi.org/10.1007/978-3-031-15255-9_6
- 807 21. Song, L., Qin, X., Hu, L.: Boomerang connectivity table revisited. applica-
808 tion to SKINNY and AES. *IACR Trans. Symmetric Cryptol.* **2019**(1), 118–
809 141 (2019). <https://doi.org/10.13154/tosc.v2019.i1.118-141>, [https://doi.org/](https://doi.org/10.13154/tosc.v2019.i1.118-141)
810 [10.13154/tosc.v2019.i1.118-141](https://doi.org/10.13154/tosc.v2019.i1.118-141)
- 811 22. Wagner, D.A.: The boomerang attack. In: Knudsen, L.R. (ed.) *Fast Software*
812 *Encryption, 6th International Workshop, FSE ’99, Rome, Italy, March 24-26,*
813 *1999, Proceedings. Lecture Notes in Computer Science, vol. 1636, pp. 156–170.*
814 *Springer (1999).* https://doi.org/10.1007/3-540-48519-8_12, [https://doi.org/10.](https://doi.org/10.1007/3-540-48519-8_12)
815 [1007/3-540-48519-8_12](https://doi.org/10.1007/3-540-48519-8_12)
- 816 23. Wang, H., Peyrin, T.: Boomerang switch in multiple rounds. application to
817 AES variants and deoxys. *IACR Trans. Symmetric Cryptol.* **2019**(1), 142–
818 169 (2019). <https://doi.org/10.13154/tosc.v2019.i1.142-169>, [https://doi.org/](https://doi.org/10.13154/tosc.v2019.i1.142-169)
819 [10.13154/tosc.v2019.i1.142-169](https://doi.org/10.13154/tosc.v2019.i1.142-169)
- 820 24. Wu, H., Huang, T.: TinyJAMBU: A Family of Lightweight Authenticated
821 Encryption Algorithms, [https://csrc.nist.gov/CSRC/media/Projects/](https://csrc.nist.gov/CSRC/media/Projects/Lightweight-Cryptography/documents/round-1/spec-doc/TinyJAMBU-spec.pdf)
822 [Lightweight-Cryptography/documents/round-1/spec-doc/TinyJAMBU-spec.](https://csrc.nist.gov/CSRC/media/Projects/Lightweight-Cryptography/documents/round-1/spec-doc/TinyJAMBU-spec.pdf)
823 [pdf](https://csrc.nist.gov/CSRC/media/Projects/Lightweight-Cryptography/documents/round-1/spec-doc/TinyJAMBU-spec.pdf), nIST LWC Round 1 Candidate, 2019
- 824 25. Wu, H., Huang, T.: TinyJAMBU: A Family of Lightweight Authenticated Encryp-
825 tion Algorithms (Version 2), [https://csrc.nist.gov/CSRC/media/Projects/](https://csrc.nist.gov/CSRC/media/Projects/lightweight-cryptography/documents/finalist-round/updated-spec-doc/tinyjambu-spec-final.pdf)
826 [lightweight-cryptography/documents/finalist-round/updated-spec-doc/](https://csrc.nist.gov/CSRC/media/Projects/lightweight-cryptography/documents/finalist-round/updated-spec-doc/tinyjambu-spec-final.pdf)
827 [tinyjambu-spec-final.pdf](https://csrc.nist.gov/CSRC/media/Projects/lightweight-cryptography/documents/finalist-round/updated-spec-doc/tinyjambu-spec-final.pdf), nIST LWC Finalist, 2021
- 828 26. Yang, Q., Song, L., Sun, S., Shi, D., Hu, L.: New properties of the double
829 boomerang connectivity table. *IACR Trans. Symmetric Cryptol.* **2022**(4), 208–
830 242 (2022). <https://doi.org/10.46586/tosc.v2022.i4.208-242>, [https://doi.org/](https://doi.org/10.46586/tosc.v2022.i4.208-242)
831 [10.46586/tosc.v2022.i4.208-242](https://doi.org/10.46586/tosc.v2022.i4.208-242)